Journal of Research in Pharmacy

Research Article

www.jrespharm.com

Novel pyrazole substituted oxazole derivatives: Design, *in-silico* studies, synthesis & biological activities

Srilakshmi SINGAGARI [1], **Raja SUNDARARAJAN** [2*]

[1] Department of Pharmaceutical Chemistry, Shadan Womens College of Pharmacy, Hyderabad – 500 004, Telangana, India.

[2] Department of Pharmaceutical Chemistry, GITAM Institute of Pharmacy, GITAM (Deemed to be University), Gandhi Nagar, Rushikonda, Visakhapatnam – 530 045, Andhra Pradesh, India.

* Corresponding Author. E-mail: sraja61@gmail.com (R.S.); Tel. +91 91605 08261.

Received: 07 October 2021 / Revised: 19 December 2021 / Accepted: 11 January 2022

ABSTRACT: A potent antibacterial drug was developed by synthesizing a set of new pyrazoles substituted oxazole derivatives using multi-step synthesis. FT-IR, ^{1}H-NMR, Mass spectroscopy, and bases of microanalyses are employed to confirm the structure of compounds. Molinspiration online tool was used to predict the molecular properties and molecular docking was used to predict the antitubercular potency of the target compounds. 10-Fold serial dilution method, agar streak dilution test, and DPPH radical scavenging methods are utilized to evaluate antitubercular, antibacterial, and radical scavenging properties of test compounds and reference drugs, respectively. Varying degree of antitubercular, antibacterial, and radical scavenging activities (mild to good) was displayed by synthesized oxazole compounds. In general, unsubstituted oxazole derivatives exhibited superior antibacterial potency than substituted analogs. In addition, meta-substituted analogs displayed higher activity than the corresponding para-substituted analogs. Among fifteen tested target compounds, the potent compound of this series was found to be 4-(4-(5-phenyl-4,5-dihydro-1*H*-pyrazol-3-yl)benzylidene)-2-methyloxazol-5(4*H*)-one (**PBO8**). Hence, this analog may be used as a lead molecule to find potent & safer antibacterial agents.

KEYWORDS: Oxazole; Pyrazole; Antitubercular activity; Antibacterial activity; Antioxidant activity.

1. INTRODUCTION

Tuberculosis (TB) is a global emergency and is amongst the worldwide health threats today. TB remains the number one killer infectious disease affecting adults in developing countries [1]. Over the last two decades, current control efforts are severely hampered due to *Mycobacterium tuberculosis* is a leading opportunistic infection in patients with acquired immune deficiency syndrome and due to the spread of multidrug-resistant strains (MDR-MTB) [2]. To address this serious health issue, continuous efforts must be devoted to identifying and developing novel drug molecules as potent antibacterial agents [3-4].

The importance of heterocyclic compounds has long been recognized in the field of synthetic organic chemistry. Currently, heterocyclic compounds have been extensively studied due to their important properties and applications. It is well known that several heterocyclic compounds containing nitrogen & oxygen exhibited a wide variety of biological activity [5]. Among these compounds, oxazole derivatives have become especially noteworthy in recent years due to their wide spectrum of biological activity such as anti-microbial [6-8], antitubercular [9-11], antioxidant [12-13], the immune regulator [14], analgesic & anti-inflammatory [15], anticancer [16] and other activities. On the other hand, pyrazoles have gained importance because of the physiological and pharmacological activities associated with them [17-21]. The antibacterial activity of pyrazole moiety is ascribed to its unique properties of being an electron donor system and ability to act as a constrained pharmacophore at the receptor site.

AutoDock tools are designed to predict the binding of small molecules with known target proteins. The active sites of the target protein, the binding energies of the small molecules are determined based on their binding mechanism. Biovia Discovery studio visualizers are used to visualize the ligand position in the enzyme binding site. This tool is very useful to study the binding nature which is useful for the development

Singagari S, Sundararajan R. Novel pyrazole substituted oxazole derivatives: Design, *in-silico* studies, synthesis & biological activities. J Res Pharm. 2022; 26(3): 625-640.

http://dx.doi.org/10.29228/jrp.160

ISSN: 2630-6344

of potential drug molecules. ADME, molecular properties, and toxicity of oxazole compounds were also evaluated by the online tool in the organic portal.

Based on the above findings and considering the wide applications of oxazoles in medicinal chemistry an attempt has been made to synthesize different oxazole derivatives containing pyrazole moiety as antibacterial agents. Oxidative stress is one of the reasons behind several disorders in which oxidants play a noteworthy role in the pathogenesis of the disease. Reactive oxygen species cause oxidative damage which is accountable for various ailments including tuberculosis & other bacterial infections. Hence, the oxazole derivatives are screened for their radical scavenging activity also.

2. RESULTS AND DISCUSSION

2.1. *Insilico* studies

2.1.1. In-silico predictions of molecular properties and ADMET

Molecular properties of the test derivatives **PBO1-PBO15** were estimated using an online molinspiration tool, in which the Lipinski rule was predicted and presented (Table 1). The results depicted that all the synthesized analogs satisfied and obey the Lipinski five rule. Entire tested compounds have only 1 to 3 hydrogen bond donors and their molecular weight is less than 500 g/mol. In addition, synthesized compounds possess only 5 to 8 hydrogen bond acceptors and their log P values are less than five. Hence, synthesized oxazole derivatives show well *in vivo* drug absorption and permeation.

Table 1: Molecular properties of synthesized compounds (PBO1-PBO15) by molinspiration

Compound code	MW (g/mol)	Log P[a]	TPSA[b]	OH-NH interact[c]	O-N interact[d]	nrotb[e]	Volume
PBO1	346.39	2.07	93.52	3	6	3	309.56
PBO2	347.37	2.52	87.72	2	6	3	306.29
PBO3	361.40	3.05	76.73	1	6	4	323.81
PBO4	345.40	3.44	67.49	1	5	3	314.83
PBO5	365.82	3.67	67.49	1	5	3	311.80
PBO6	410.27	3.80	67.49	1	5	3	316.15
PBO7	376.37	2.95	113.32	1	8	4	321.60
PBO8	331.38	3.00	67.49	1	5	3	298.27
PBO9	346.39	2.05	93.52	3	6	3	309.56
PBO10	347.37	2.49	87.72	2	6	3	306.29
PBO11	361.40	3.03	76.73	1	6	4	323.81
PBO12	345.40	3.42	67.49	1	5	3	314.83
PBO13	365.82	3.65	67.49	1	5	3	311.80
PBO14	410.27	3.78	67.49	1	5	3	316.15
PBO15	376.37	2.93	113.32	1	8	4	321.60

[a] Calculated octanol/water partition coefficient; [b] Molecular polar surface area; [c] Number of hydrogen-bond donors; [d] Number of hydrogen-bond acceptors; [e] Number of rotatable bonds.

The selection of prime potential drug molecules was consolidated as a therapeutic agent. However, those may fail in clinical trials and exist adverse effects. Hence, in the drug discovery process to predict the reach of synthesized compounds into the target site the essential parameter used is pharmacokinetic parameters. Table 2 data shows the ADME properties of synthesized derivatives by their significant results. *In silico* ADME predictions clearly show that the proposed analogs penetrate the Blood-Brain Barrier to a negligible extent only. CaCo-2 cell and MDCK cell permeability of the test compounds are considerably low. The tested compounds were absorbed well in the human intestine and bonded with plasma protein. Hence, synthesized compounds possess drug-likeness properties.

http://dx.doi.org/10.29228/jrp.160
J Res Pharm 2022; 26(3): 625-640

Table 2: ADME properties and drug-likeness scores of the synthesized compounds **(PBO1-PBO15)**

Compound code	BBB[a]	PPB [b]	HIA [c]	CaCo-2 [d]	MDCK [e]
PBO1	0.017	79.56	95.12	19.99	17.12
PBO2	0.027	85.27	94.15	20.03	13.97
PBO3	0.023	86.60	96.35	26.49	14.48
PBO4	0.026	89.36	96.03	25.92	27.85
PBO5	0.031	89.96	96.25	23.81	15.26
PBO6	0.033	94.64	96.53	23.92	9.03
PBO7	0.053	87.19	95.27	19.45	10.58
PBO8	0.020	89.16	96.00	24.67	10.14
PBO9	0.015	80.60	95.12	19.78	11.85
PBO10	0.026	85.94	94.15	19.42	10.80
PBO11	0.020	87.31	96.35	26.05	10.46
PBO12	0.026	88.88	96.03	25.97	10.77
PBO13	0.030	90.71	96.25	23.49	11.59
PBO14	0.032	90.19	96.53	23.75	9.02
PBO15	0.121	88.52	95.27	17.00	10.47

[a] Blood-Brain Barrier penetration; [b] Plasma protein binding; [c] Human intestinal absorption; [d] CaCo-2 cell permeability; [e] MDCK cell permeability

The toxicity prediction of target compounds was also reported (Table 3), in which the mutagenic property of the test compounds was assessed using the Ames test. In general Ames test was employed to determine whether the tested chemical agent causes DNA mutations or not in bacteria. From the reports of the Ames test, it was found that the majority of the test compounds were non-mutagenic. In addition, mouse and rat carcinogenicity were also predicted and found that by nature most of the test analogs didn't exhibit carcinogenicity.

Table 3: Toxicity prediction of synthesized compounds **(PB01-PB15)**

Compound code	Ames test mutagenicity	Mouse carcinogenicity[a]	Rat carcinogenicity[b]
PBO1	Non-Mutagen	Positive	Positive
PBO2	Mutagen	Positive	Positive
PBO3	Non-Mutagen	Positive	Positive
PBO4	Non-Mutagen	Positive	Negative
PBO5	Non-Mutagen	Positive	Positive
PBO6	Non-Mutagen	Positive	Negative
PBO7	Mutagen	Positive	Positive
PBO8	Non-Mutagen	Positive	Negative
PBO9	Mutagen	Positive	Negative
PBO10	Non-Mutagen	Negative	Positive
PBO11	Non-Mutagen	Negative	Negative
PBO12	Non-Mutagen	Positive	Positive
PBO13	Mutagen	Positive	Positive
PBO14	Mutagen	Positive	Positive
PBO15	Non-Mutagen	Positive	Positive

[a]Positive = No carcinogenicity in mouse; [b]Positive = No carcinogenicity in rats; [a]Negative = Carcinogenicity in mouse; [b]Negative = Carcinogenicity in rats

In the drug discovery process, the physicochemical properties, pharmacokinetics, and toxicity studies of tested drugs are essential for qualifying in clinical trials. On this aspect, the molecular properties of the synthesized derivatives were predicted in molinspiration online tools. Based on the Lipinski rule, molecular weight, hydrogen donor/acceptor, and non-rotational bonds of the synthesized motifs produced their affordable result towards their molecular properties [22]. Additionally, the polar surface area was also showed significant value, which is accountable for their oral bioavailability. Transport characteristics of molecules like blood-brain barrier penetration and intestinal absorption were determined from molecular volume. Often in QSAR studies volume is therefore used to denote the relationship between molecular properties and biological

http://dx.doi.org/10.29228/jrp.160
J Res Pharm 2022; 26(3): 625-640

activity. Based on the existing literature, these afforded values were referred [23]. Based on the results of the Lipinski rule and ADMET the synthesized motifs were optimized for further studies.

By using pre-ADMET tools pharmacokinetic parameters such as adsorption, distribution, metabolism, and excretion were analyzed. From the study, it was found that tested compounds were extremely absorbed by the human intestine as well as bonded on plasma protein for distribution. The low absorption on the blood-brain barrier indicated that these analogs were orally active drugs but CNS inactive agents. Generally, low molecular weight analogs pass by absorption through CNS as it is composed of connective tissues over the capillaries. The tested analogs possessed poor absorption in the blood-brain barrier in the range of 0.1 to 0.01 values. Even though drug molecules are highly absorbed in the intestine, protein binding generally decreases the BBB absorption due to the minimum content of drug molecules in circulation. In addition to the drug action, plasma protein binding also gives information about the efficacy and disposition of drugs. The tested derivatives were found as strongly bound chemicals as it possesses more than 87 % of results. Test compounds showed more than 93 % absorption which indicates the high absorption of test scaffolds in the human intestine. In oral active absorption prediction, most of the tested analogs showed below 52 % which indicates the medium range of permeability and very few compounds showed below 4 % which indicates less permeability. The tested analogs were found to be orally active and hence enhanced the bioavailability from their 19 to 35 % moderate permeability.

2.1.2. Molecular docking study

From the targeted molecular simulations, it was found that the oxazole analogs produced significant results in all tested targets and the obtained results are presented in Table 4. The docking score for synthesized derivatives **(PBO1-PBO15)** on MtKasA (PDB ID: 2WGE) produced significant results in the range of **-7.52 to -9.94** Kcal/mole compared with native control inhibitor and isoniazid were **-7.9** and **-4.59** Kcal/mole. Among the fifteen compounds, **PB12** was afforded highly significant results as **-9.94** Kcal/mole and produced its potency through binding affinity towards the targeted enzyme by hydrophilic and hydrophobic interactions were shown in Figures 1A & 1B.

Table 4. Docking score of synthesized compounds **(PB01-PB15)** on MtKasA

Ligands	Docking score (kcal/mole) MtKasA (2WGE)	Binding Site Amino Acid Residues	
		Hydrogen Bond Interactions	Hydrophobic Bond Interactions
PBO1	-8.12	Asp A:273 and Asn A:402	Pro A: 280; Gly A:318 and Ile A:317.
PBO2	-7.52	Glu A:203	Ile 347; Leu 205; Phe 239; Pro 206 and Gly 118.
PBO3	-8.43	Gly A:118	His A:345; Pro A: 206; Ile A: 202; Phe A:239, Glu A: 203 and Val A:123.
PBO4	-8.39	Gly A:203	Phe A:239; Ile A:202; Ala A:204; Leu A:205; Pro A:206 and Gly A:118.
PBO5	-9.67	Ile A:317; Thr A:315 and Gly A:318	Arg A:214; Ala A:215, 280, 287, 321, 325 and Phe A:402.
PBO6	-8.61	Met A:213	Arg A:214; Ala A;215, 279; Ile A:317; Pro A:280 and Phe A:404.
PBO7	-8.24	Gly A:203	Gly A:118; Ile A:202; Ala A:204; Leu A:205; Pro A:206 and Phe A:239.
PBO8	-9.21	Ile A: 317 and Gly A:318	Arg A:214; Ala A:279; Pro A:280 and 316.
PBO9	-8.66	Val A:278, 279 and Ile A: 317	Arg A:214; Ala A:215 and Pro A:280
PBO10	-9.18	Pro A:201; Glu A:203; Ala A:204 and Leu A:205.	Glu A:199 and Pro A:206.
PBO11	-9.04	Pro A:201 and Leu A:205.	Gly A:200; Ile A:202 and Pro A:206.
PBO12	-9.94	Gly A:318	Arg A:214; Ala A:215, 321; Pro A:280, 316 and Phe A:402.
PBO13	-9.33	Pro A:201; Ala A:204 and Leu A:205.	Ile A:202; Pro A:206 and Phe A:239
PBO14	-8.97	Pro A:201	Val A:123; Ile A:202; Glu A:203 and Pro A:206.
PBO15	-8.26	Pro A:201 and Leu A:205.	Pro A:206 and Ile A:202

http://dx.doi.org/10.29228/jrp.160
J Res Pharm 2022; 26(3): 625-640

Control inhibitor - Thiolactomycin	**-7.9**	Gln 93	-
Isoniazid	**-4.59**	Met A:144; Ser A:81 and Gly A:118.	Gly A:117 and Pro A:117.

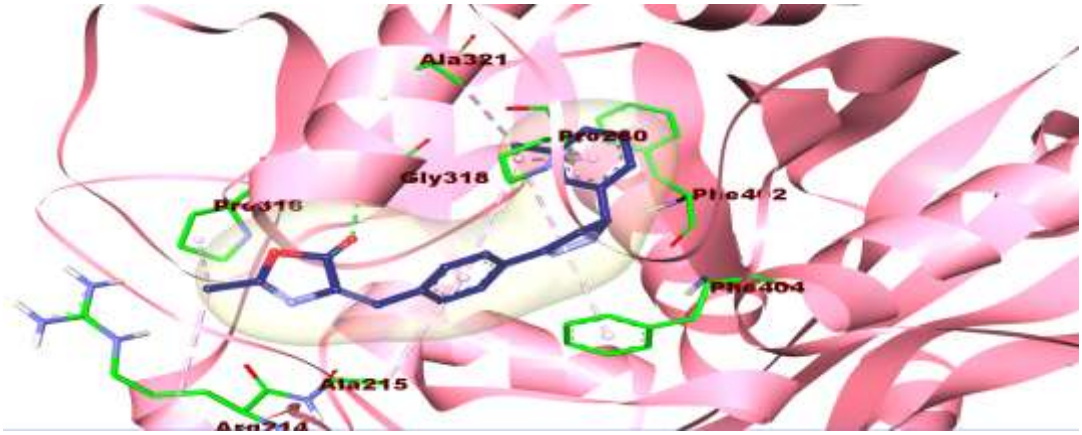

Figure 1A: Molecular interactions between PBO12 and MtKasA by Biovia discovery studio visualizer (Docked pose of PBO12 and MtKasA binding site)

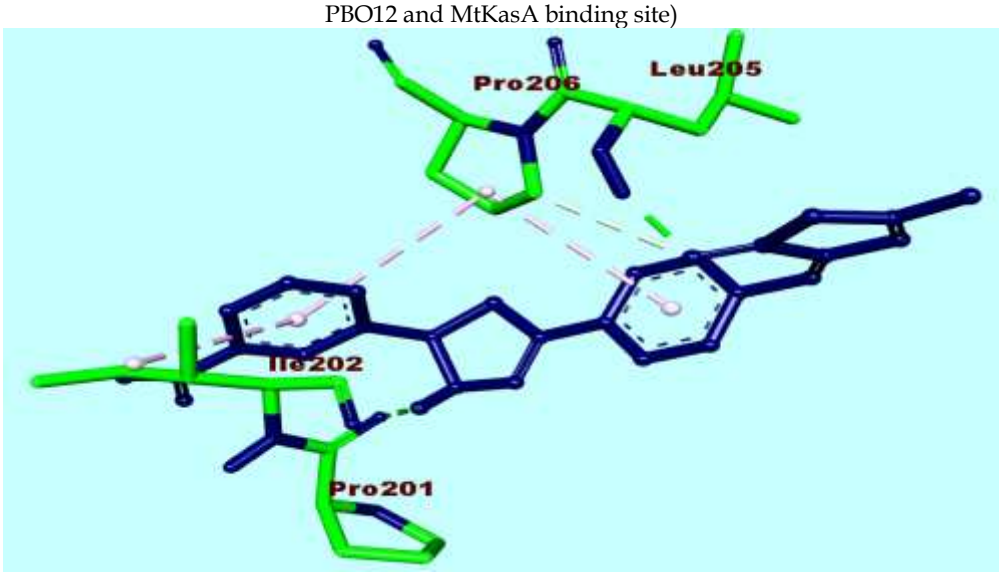

Figure 1B: Hydrogen bond interactions on PBO12 and MtKasA (green dashed lines) and Hydrophobic bonds (Pink dashed lines) and other amino acid residues.

The second target of molecular docking study is **MtpKnB** (Serine/threonine-protein kinase – B), in which all tested derivatives were found to be noteworthy binding affinity towards this receptor. Among these, **PBO8** and **PBO10** showed high binding scores such as -8.61 & -8.91 kcal/mole, respectively compared with control inhibitor mitoxantrone (-8.19 Kcal/mole) and isoniazid (-3.93 Kcal/mole). The results were mentioned in Table 5 and the binding pose of **PB10 is** represented in Figures 2A & 2B.

Table 5: Docking score of synthesized compounds **(PBO1-PBO15)** on MtpKnB

Ligands	Docking score (kcal/mole) MtpKnB (2FUM)	Binding Site Amino Acid Residues	
		Hydrogen Bond Interactions	**Hydrophobic Bond Interactions**
PBO1	-8.0	Ser B:8 and His B:6.	Pro B:4 and 84.
PBO2	-7.9	Glu B:81	Pro B:4, 83; Thr B:3 and Ala C:238.
PBO3	-8.14	Glu B:81 and Thr B:3	Pro B:4; Ala C:84 and 238.
PBO4	-8.39	Glu B:81and His B:36	Ala C: 238; Pro B: 4 and Arg C:239.
PBO5	-8.23	Glu B:81; Ser B:8 and His B:6	Arg C: 239; Ala C: 238 and Pro B:4.

http://dx.doi.org/10.29228/jrp.160
J Res Pharm 2022; 26(3): 625-640

PBO6	-8.7	Ser B:8 and Glu B:81	Ala C:238; Pro B:4 and 3.
PBO7	-7.76	Arg C:230; Arg A:137 and 55.	Arg A:161; Leu A:54; Ala C:225 and Val C:229.
PBO8	-8.61	Glu B:81 and His B:6	Ala C:28; Pro B:4 and 83.
PBO9	-8.31	Glu B:81 and Thr B:82	Pro B:4
PBO10	**-8.91**	Ala B: 84 and Thr B:82.	Pro B:4 and 83.
PBO11	-8.06	Ser B: 5 and His B:6.	Ala B:80; Pro B:4 and 83.
PBO12	-8.07	His B:6 and Ser C:237	Ala C:238; Ala B:80 and Pro B:4
PBO13	-8.58	Glu B:81	Ala C:238; Ala B:84; Pro B:4 and 83.
PBO14	-8.74	Ser B:15 and Glu B:81	Ala C:238 and Pro B:4
PBO15	-8.31	Glu B:81; Thr B: 82 and Ala B:84.	Ala C:238; Thr B:3 and Pro B:4.
Control inhibitor - Mitoxantrone	**-8.19**	Lys A:140; Asn A:143 and Val A:95.	Phe A:19; Leu A:17; Gly A:97; Asp A:102; Met A:92, 145 and 155; Ala A : 38 and Val A:25.
Isoniazid	**-3.93**	Ala A:64; Tyr A:75 and 94.	Arg A:35 and Ala A:65.

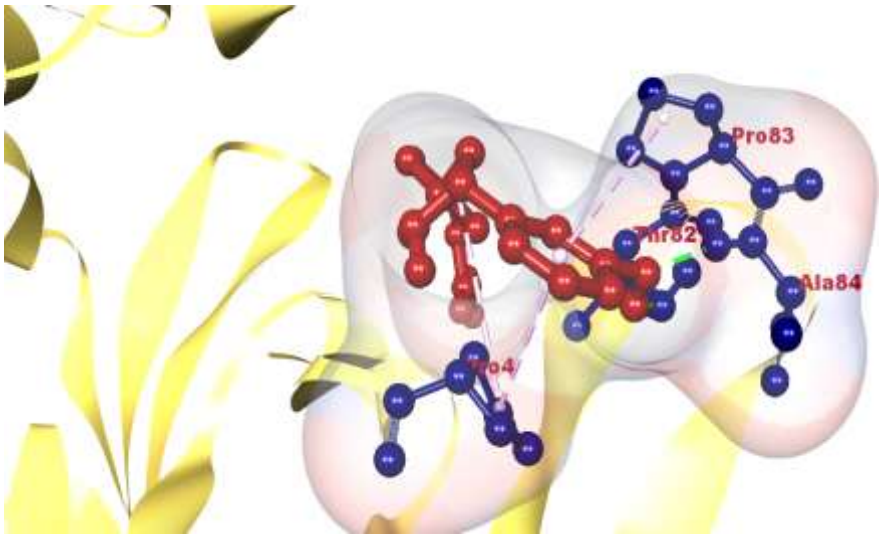

Figure 2A: Molecular interactions between **PBO10** and MtpKnB by Biovia discovery studio visualizer (Docked pose of PBO10 and MtpKnB binding site)

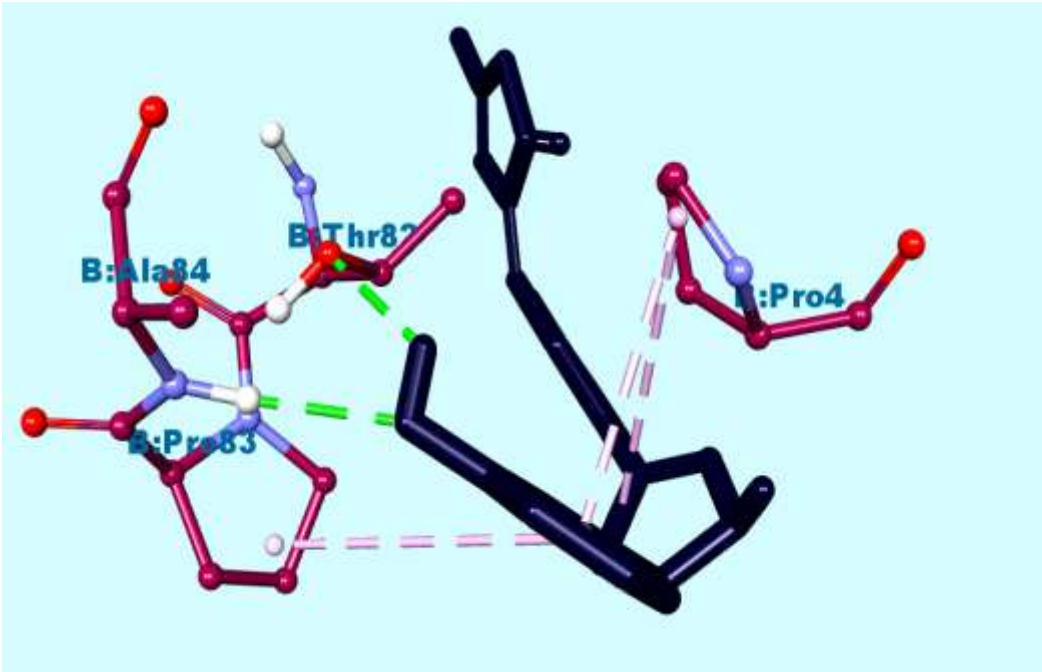

http://dx.doi.org/10.29228/jrp.160
J Res Pharm 2022; 26(3): 625-640

Figure 2B: Hydrogen bond interactions on **PBO10** and MtpKnB (green dashed lines) and Hydrophobic bonds (Pink dashed lines) and other amino acid residues**.**

In the present research, the anti-TB potential range of synthesized derivatives was investigated to characterize their affinity towards MtKasA using a guided molecular docking approach. MtKasA is a key enzyme necessary for the growth and survival of *M. tuberculosis* which is the rationale behind the selection of this particular protein. In addition, this protein is also involved in many essential mycobacterial pathways like cofactor biosynthesis, cell wall biogenesis, and signal transduction. In mammalian cells this enzyme is absent; hence, for mycobacterial diseases, it is highly selective and attractive 'druggable' targets. At present no marketed drug is available against this newly validated emerging target. The complex structure of the mycobacterium cell wall is composed of arabinogalactan, peptidoglycan, lipoarabinomannan, and some mycolic acids. In this study *β-ketoacyl acyl carrier protein synthase*, I (MtKasA) was used, which is responsible for *M. tuberculosis* cell wall biosynthesis. The mycobacterial cell wall is composed of mycolic acid which is a unique feature. In the host, mycolic acid is responsible for the survival of mycobacteria and it is synthesized using a variety of *fatty acid synthase (FAS)*. MtKasA is only found in bacteria and the mycobacterial type II *FAS* pathway it is one of the enzymes. Protein kinase B (MtPknB) comes under serine/threonine protein kinases are another target. In signal transduction pathways it plays a major role and is also involved in the mycobacterial cell morphology regulation. Hence, it allows the growth and survival of *M. tuberculosis* within the host [24-25].

The main aim of molecular docking is to utilize scoring algorithms to evaluate the probability of synthesized compounds binding to targeted protein. Hence, the study identified that among the synthesized motifs **PBO10** and **PBO12** produced high binding affinity towards both proteins (2wfe and 2fum) than control inhibitors, thiolactomycin, and mitoxantrone, respectively.

2.2. Synthesis and characterization

A novel pyrazole substituted oxazoles (**PBO1-PBO15)** were prepared as per the protocol stated in the Scheme. Fifteen different substituted pyrazole benzylidenes are placed at the C-4 position of 2-methyloxazol-5(4*H*)-one to synthesize oxazole compounds (**PBO1-PBO15)**. In this research work, fifteen novel 4-(4-(5-(substituted phenyl)-4,5-dihydro-1*H*-pyrazol-3-yl)benzylidene)-2-methyloxazol-5(4*H*)-one (**PBO1-PBO15**) were prepared from acetyl glycine & 4-acetylbenzaldehyde by a multi-step synthesis. Initially, acetyl glycine was cyclized with 4-acetylbenzaldehyde in presence of acetic anhydride and sodium acetate to produce 4-(4-acetylbenzylidene)-2-methyloxazol-5(4*H*)-one (**ABO**). Later, the synthesized 4-(4-acetyl benzylidene)-2-methyloxazol-5(4*H*)-one (**ABO**) was reacted with a different aromatic aldehyde in presence of a catalytic quantity of sodium hydroxide and produced corresponding chalchones i.e., 4-(4-(3-(substituted phenyl)acryloyl)benzylidene)-2-methyloxazol-5(4*H*)-one (**CBO1-CBO15**). Finally, the obtained chalcones **(CBO1-CBO15)** were treated with hydrazine hydrate to synthesize target compounds i.e., 4-(4-(5-(substituted phenyl)-4,5-dihydro-1*H*-pyrazol-3-yl)benzylidene)-2-methyloxazol-5(4*H*)-one (**PBO1-PBO15**) through simple cyclization reaction. TLC was employed for the reaction optimization, completion, and purity of the prepared oxazole and intermediate derivatives [26].

http://dx.doi.org/10.29228/jrp.160
J Res Pharm 2022; 26(3): 625-640

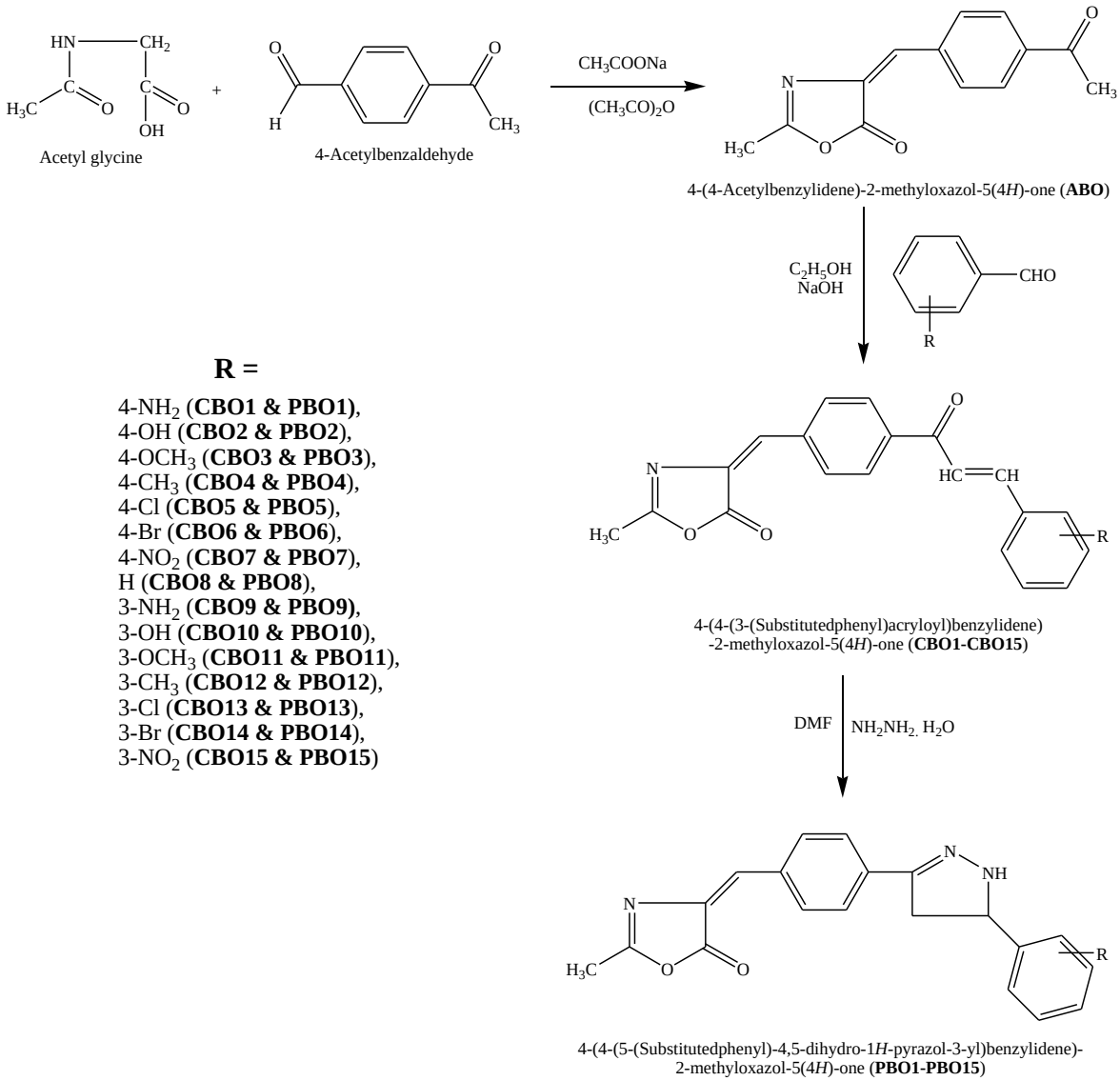

Scheme: Synthetic scheme for synthesis of title compounds (PBO1-PBO15)

The chemical structure of the prepared intermediates and target compounds are confirmed from various spectroscopic techniques such as IR, ^{1}H-NMR, mass spectra, and microanalysis. Spectral studies of all compounds confirm the assigned structures. Characteristic absorption peaks present in IR spectra represent the presence of some specific groups in chemical structure. In IR spectrum of 4-(4-acetylbenzylidene)-2-methyloxazol-5(4*H*)-one (**ABO**), the appearance of the absorption peak at 3084 cm^{-1} corresponds to alkene =CH stretching & disappearance of absorption peak around 3500 & 3300 cm^{-1} corresponds to carboxylic acid and amino group, respectively confirms its formation. It is further supported by the appearance of a singlet peak in the NMR spectrum at δ 7.90 ppm corresponds to =CH of oxazole. IR spectrum of 4-(4-(3-(substituted phenyl)acryloyl)benzylidene)-2-methyloxazol-5(4*H*)-one (**CBO1-CBO15**) displayed the following common absorption bands: a) 1206-1269 cm^{-1} (C-O-C stretching), b) 1600-1640 cm^{-1} (C=C stretching), c) 1640-1667 cm^{-1} (C=N stretching), d) 1731-1758 cm^{-1} (C=O stretching), e) 2903-2958 cm^{-1} (Aliphatic C-H stretching), f) 3001-3027 cm^{-1} (Aromatic C-H stretching) and g) 3050-3097 cm^{-1} (Alkene =CH stretching). The formation of **CBO1-CBO15** was confirmed from the NMR spectrum by the appearance of two doublet peaks for a single proton around δ 8.00 ppm corresponds to COCH=CH [26].

The appearance of IR absorption peak at 3350-3433 cm^{-1} corresponds to N-H stretching confirms the formation of oxazole compounds i.e., 4-(4-(5-(substituted phenyl)-4,5-dihydro-1H-pyrazol-3-yl)benzylidene)-2-methyloxazol-5(4*H*)-one (**PBO1-PBO15**). It is further supported by the appearance of a doublet peak for two protons of pyrazole CH_2 between δ 1.54-2.49 ppm, triplet for a single proton of pyrazole CH between δ 3.48-4.47 ppm and singlet peak for one proton of pyrazole NH at δ 7.79-8.59 ppm in the NMR spectrum. Additionally, IR spectrum of 4-(4-(5-(substituted phenyl)-4,5-dihydro-1H-pyrazol-3-yl)benzylidene)-2-

http://dx.doi.org/10.29228/jrp.160
J Res Pharm 2022; 26(3): 625-640

methyloxazol-5(4*H*)-one (**PBO1-PBO15**) displayed the following common absorption bands: a) 1202-1258 cm^{-1} (C-O-C stretching), b) 1602-1648 cm^{-1} (C=C stretching), c) 1641-1668 cm^{-1} (C=N stretching), d) 1733-1759 cm^{-1} (C=O stretching), e) 2900-2959 cm^{-1} (Aliphatic C-H stretching), f) 3001-3026 cm^{-1} (Aromatic C-H stretching) and g) 3037-3098 cm^{-1} (Alkene =CH stretching). The following common peaks are observed in ^{1}H-NMR spectra of target analogs **PBO1-PBO15**: a) Singlet between δ 0.82-1.53 ppm for 3 protons corresponds to CH_3 of oxazole; b) Multiplet between δ 6.72-8.29 ppm for eight or nine aromatic C-H protons. c) Singlet between δ 7.94-8.98 ppm for one proton corresponds to =CH of oxazole.

Moreover, compounds **CBO1 & CBO9** displayed an absorption peak around 3300 cm^{-1} corresponding to N-H stretching. Compounds **CBO2, CBO10, PBO2 & PBO10** displayed an absorption peak of around 3400 cm^{-1} corresponding to O-H stretching. Compounds **CBO5, CBO13, PBO5 & PBO13** showed a peak around 700 cm^{-1} corresponding to C-Cl stretching, and Compounds **CBO6, CBO14, PBO6 & PBO14** showed a peak around 600 cm^{-1} corresponds to C-Br stretching. Nitro group present in oxazole compounds **CBO7, CBO15, PBO7 & PBO15** is confirmed by the appearance of two characteristic peaks around 1550 cm^{-1} & 1350 cm^{-1} in IR. Further purity and molecular weight of the prepared analogs were confirmed their mass spectral analysis. In addition, microanalysis reports are also within the limit which further supports the proposed chemical structure of the synthesized analogs.

2.3. Biological activities

2.3.1. Antitubercular activity

In-vitro antitubercular potency of all target analogs was screened against *M. tuberculosis* (H_{37}Rv strain) and MIC of entire tested analogs were determined and presented in Table 6. Simultaneously MIC of INH, rifampicin, and ethambutol was also measured to control the test organism sensitivity. From the reports, it was found that in varying degrees synthesized derivatives inhibited the growth of *M. tuberculosis*. Amongst various tested analogs, **PBO10 & PBO12** inhibited the growth of *M. tuberculosis* at a low concentration (MIC: 3.13 µg/ml) compared to reference standard such as isoniazid (MIC: 0.05 µg/ml), rifampicin (MIC: 0.10 µg/ml) and ethambutol (MIC: 1.56 µg/ml). These derivatives possess hydroxy and a methyl group at the meta position of the phenyl ring attached at the 5th position of pyrazole. MIC of test compounds **PBO8, PBO13,** and **PBO14** was found to be 6.25 µg/ml may be due to the presence of hydrogen, chloro, and bromo group in the phenyl ring, respectively. In addition, compounds **PBO9** & **PBO11** containing amino/methoxy group in phenyl ring completely inhibited the growth of *M. tuberculosis* at 12.5 µg/ml concentration. The MIC of remaining synthesized analogs (**PBO1 – PBO7 & PBO15**) were found to be 25 µg/ml.

2.3.2. Antibacterial activity

In vitro, an agar streak dilution technique was employed to screen the antibacterial potency of test derivatives **PBO1-PBO15**. Simultaneously MIC of Ciprofloxacin was also measured to control the test organism sensitivity. MIC of standard and test analogs was compared effectively in Table 6. Antibacterial data indicate that all tested analogs showed variable degrees of potency. In this research, overall, it was found that oxazole analog (**PBO8**) exhibited good antibacterial activity; target analogs (**PBO12-PBO14**) showed moderate antibacterial activity; whereas all other oxazole analogs (**PBO1- PBO7, PBO9- PBO11 & PBO15**) produced only reduced antibacterial activity. The presence of hydrogen in the phenyl ring might be responsible for the powerful antibacterial activity displayed by the derivative (**PBO8**). In general, from this research, it was found that unsubstituted target derivatives (**PBO8**) exhibited superior antibacterial potency than substituted analogs (**PBO1-PBO7 & PBO9-PBO15)**. Within substituted analogs, it was found that the position of the substituent plays a significant role in antibacterial activity than the nature of the substituent. Meta-substituted analogs (**PBO9-PBO15**) showed higher activity than the corresponding para-substituted analogs (**PBO1-PBO7**). The nature of the substituent doesn't play a major role in antibacterial activity as both electron-donating and withdrawing groups containing target compounds displayed similar activity. Among fifteen tested oxazole compounds the potent compound of this series was found to be 4-(4-(5-phenyl-4,5-dihydro-1*H*-pyrazol-3-yl)benzylidene)-2-methyloxazol-5(4*H*)-one (**PBO8**). Tests analog **PBO8** exhibited equipotent activity to Ciprofloxacin against *B. subtilis* (MIC: 1.56 µg/ml), *S. epidermidis* (MIC: 3.13 µg/ml), *S. albus* (MIC: 1.56 µg/ml), and *P. vulgaris* (MIC: 1.56 µg/ml). In addition, this analog also displayed comparable antibacterial activity against the rest of the tested microorganisms such as *S. aureus, M. luteus*, *S. typhimurium, K. pneumonia P. aeruginosa* and *E. coli*.

http://dx.doi.org/10.29228/jrp.160
J Res Pharm 2022; 26(3): 625-640

Journal of Research in Pharmacy
Research Article
www.jrespharm.com

Table 6: MIC (Minimum inhibitory concentration in µg/ml) of synthesized target compounds (PBO11-PBO1515) & standard drugs.

Compounds code	*M. tuberculosis*	*B. subtilis*	*S. aureus*	*S. epidermidis*	*S. albus*	*M. luteus*	*S. typhimurium*	*K. pneumoniae*	*P. vulgaris*	*P. aeruginosa*	*E. coli*
PBO1	25	100	100	100	50	50	100	50	100	50	50
PBO2	25	50	50	100	50	50	100	50	50	50	25
PBO3	25	50	25	50	50	25	50	50	50	25	25
PBO4	25	25	25	50	25	50	50	25	25	50	25
PBO5	25	25	12.5	25	25	12.5	50	25	12.5	25	12.5
PBO6	25	25	25	12.5	25	25	25	25	25	50	12.5
PBO7	25	100	50	50	100	50	100	100	100	50	100
PBO8	6.25	1.56	3.13	3.13	1.56	3.13	6.25	3.13	1.56	3.13	6.25
PBO9	12.5	12.5	6.25	12.5	12.5	12.5	12.5	6.25	6.25	12.5	12.5
PBO10	3.13	6.25	12.5	12.5	12.5	6.25	12.5	12.5	6.25	12.5	6.25
PBO11	12.5	6.25	6.25	12.5	6.25	6.25	12.5	6.25	3.13	12.5	6.25
PBO12	3.13	6.25	6.25	6.25	3.13	6.25	6.25	12.5	3.13	6.25	12.5
PBO13	6.25	3.13	3.13	3.13	1.56	6.25	6.25	3.13	3.13	6.25	6.25
PBO14	6.25	3.13	3.13	6.25	3.13	3.13	6.25	6.25	1.56	3.13	6.25
PBO15	25	12.5	12.5	25	12.5	12.5	25	12.5	12.5	25	12.5
Isoniazid	0.05	-	-	-	-	-	-	-	-	-	-
Rifampicin	0.10	-	-	-	-	-	-	-	-	-	-
Ethambutol	1.56	-	-	-	-	-	-	-	-	-	-
Ciprofloxacin	-	1.56	1.56	3.13	1.56	1.56	3.13	1.56	1.56	1.56	3.13

Singagari S, Sundararajan R. Novel pyrazole substituted oxazole derivatives: Design, *in-silico* studies, synthesis & biological activities. J Res Pharm. 2022; 26(3): 625-640.

ISSN: 2630-6344
http://dx.doi.org/10.29228/jrp.160

2.3.3. Antioxidant screening (DPPH radical scavenging activity)

The anti-oxidant screening results of were presented in Table 7. DPPH (1,1-diphenyl-2-picryl-hydrazine) radical scavenging technique is widely and conveniently used to measure antioxidant efficacy because it is considered a good *in-vitro* technique. At 517 nm, DPPH is absorbed in its radical form, but it disappeared when antioxidant radical or compound reduces DPPH. Hence, the purple color changes to yellow color. The hydrogen donating ability of the prepared analogs is indicated by this color change. 1,1-Diphenyl-2-picrylhydrazine is produced when antioxidants are reacting with DPPH. At five different concentrations, the oxazole compounds are treated for 30 min with free stable DPPH radical to estimate the reducing abilities of the target compounds. The maximum scavenger potency was observed in derivatives **PBO13** & **PBO14** which may be due to the presence of chloro/bromo moiety in the phenyl ring. IC_{50} of **PBO13** & **PBO14** was found to be 562.74 & 587.43 µg/ml compared to reference ascorbic acid (IC_{50}: 330.27 µg/ml). The moderate antiradical activity was shown by compounds **PBO5** & **PBO6** & **the** rest of the tested derivatives exhibited weaker antiradical activity. Generally, the electron-withdrawing group (nitro, chloro, and bromo) containing compounds exhibited better antiradical activity than the electron-donating group (amino, hydroxy, methoxy & methyl) containing compounds. In addition, the presence of substituent at meta position exhibited slightly better activity than ortho position.

Table 7: DPPH radical scavenging activity (expressed as % inhibition & IC_{50}) of synthesized compounds **(PBO1–PBO15)**

Compounds code	% Inhibition					Regression analysis		IC_{50} Value
	200 µg/ml	400 µg/ml	600 µg/ml	800 µg/ml	1000 µg/ml	Equation	R^2	
PBO1	11.61	18.40	22.03	27.95	36.55	y = 0.0297x + 5.479	0.9826	1499.02
PBO2	12.93	15.34	22.79	30.01	37.42	y = 0.0318x + 4.603	0.9768	1427.58
PBO3	14.99	28.32	36.75	40.14	48.94	y = 0.0399x + 9.912	0.9601	1004.71
PBO4	16.50	24.29	37.83	44.00	51.53	y = 0.0449x + 7.899	0.9839	937.66
PBO5	25.34	39.16	50.70	57.52	72.08	y = 0.0559x + 15.408	0.9890	618.82
PBO6	26.82	35.74	48.61	59.07	70.79	y = 0.0556x + 14.825	0.9977	632.64
PBO7	20.64	36.16	45.09	54.83	64.62	y = 0.0533x + 12.279	0.9883	707.71
PBO8	25.75	32.90	40.78	49.58	59.32	y = 0.0419x + 16.52	0.9962	799.05
PBO9	10.87	17.65	23.02	29.46	40.15	y = 0.0352x + 3.119	0.9824	1331.85
PBO10	12.63	19.08	26.54	33.79	44.93	y = 0.0397x + 3.601	0.9886	1168.74
PBO11	15.31	23.70	36.92	42.24	50.61	y = 0.0446x + 7.014	0.9841	963.81
PBO12	18.64	27.89	38.30	45.71	52.05	y = 0.0423x + 11.126	0.9909	919.01
PBO13	29.17	42.81	50.93	64.05	73.26	y = 0.0547x + 19.218	0.9944	562.74
PBO14	27.34	38.61	52.08	63.90	71.57	y = 0.0569x + 16.575	0.9926	587.43
PBO15	23.78	37.65	44.87	56.28	65.80	y = 0.0513x + 14.875	0.9926	684.70
Vitamin - C	42.80	56.38	63.71	79.23	98.69	y = 0.0673x + 27.773	0.9764	330.27

3. CONCLUSION

A variety of novel pyrazole substituted oxazole derivatives were synthesized by multistep synthesis. FT-IR, ^{1}H-NMR, Mass spectroscopy & microanalysis are performed to confirm the chemical structure of all prepared intermediate and target derivatives. The molecular properties of the synthesized derivatives were predicted in molinspiration online tools. The anti-TB potential range for synthesized derivatives was estimated by a guided molecular docking approach to characterize their affinity towards MtKasA and MtpKnB. *In vitro,* antitubercular and antibacterial activities of all novel analogs were estimated by measuring their MIC. In addition, the antioxidant potency of analogs was tested using DPPH radical scavenging method. Synthesized oxazole compounds displayed a varying degree of antitubercular, antibacterial, and antioxidant activities (mild to good). In general, from this research, it was found that unsubstituted target derivatives (PBO8) exhibited superior antibacterial potency than substituted analogs (PBO1-PBO7 & PBO9-PBO15). Within substituted analogs, it was found that the position of the substituent plays a significant role in antibacterial activity than the nature of the substituent. Meta-substituted analogs (PBO9-PBO15) showed higher activity than the corresponding para-substituted analogs (PBO1-PBO7). Among fifteen tested target compounds the potent compound of this series was found to be 4-(4-(5-phenyl-4,5-dihydro-1*H*-pyrazol-3-yl)benzylidene)-2-

Singagari S, Sundararajan R. Novel pyrazole substituted oxazole derivatives: Design, *in-silico* studies, synthesis & biological activities. J Res Pharm. 2022; 26(3): 625-640.

http://dx.doi.org/10.29228/jrp.160
ISSN: 2630-6344

methyloxazol-5(4*H*)-one (PBO8). This derivative displayed potent antitubercular and antibacterial activities and moderate antioxidant activity. For this reason, this compound could be extended as a new class of antitubercular and antibacterial drugs. On the other hand, more structural modification is planned to improve the antitubercular and antibacterial potency.

4. MATERIALS AND METHODS

4.1. Materials

The reagents and chemicals utilized in this research were procured from several industries like CDH, SD Fine Chem., Qualigens, and E. Merck India Ltd. LR grade solvents were used with purification before their use. From E. Merck India Ltd., silica gel G was obtained for TLC (analytical chromatography). Using open glass capillary melting points of synthesized compounds were measured and are uncorrected. Jasco FT-IR 410 spectrometer was used to record the IR spectra of synthesized compounds in KBr pellets. ^{1}H-NMR spectra of synthesized derivatives were measured on Bruker FT-NMR spectrometer at 300 MHz. TMS (tetramethylsilane) was used as an internal standard for ^{1}H-NMR and on ppm scale, the chemical shifts are documented. Electron impact ionization was used to measure the mass spectra using the JEOL-SX-102 instrument. 2400C analyzer model from Perkin Elmer was utilized for recording microanalysis.

4.1.1. Software required

From www.scripps.edu, AutoDock 4.2 and MGL (molecular graphics laboratory) tools were downloaded. Chemdraw ultra for sketching and chem 3D Pro for energy minimization and convert chem draw file into pdb format. Molegro Molecular viewer (http://molexus.io/molegro-molecular-viewer) from which protein can be pre-processed, binding pocket interactions can be accessed, the docked complex can be explored.

4.1.2. Predictions of physicochemical properties and ADMET

In the drug discovery process, physicochemical properties by 5-Lipinski's rule were observed for predicting the bioactive drug in the oral route [27]. In pharmacokinetic studies, screening of ADME properties is evaluated for understanding their bioavailability [28]. Additionally, molecular properties and toxicity were evaluated by the online tool in the organic portal web of preADMET and molinspirations [29].

4.1.3. Molecular docking

Computer-aided drug design is one of the tools which plays a vital role in understanding the structure-activity relationship, binding energy, the interaction between the protein and ligand, binding affinity, etc. In this program, Auto dock was widely used in evaluating the binding studies of our ligand (synthesized compound **PBO1-PBO15**) with our target enzymes. This program helps us to predict how these small molecules of synthesized derivatives may bind with the targeted enzyme MtKasA (ID of PDB: 2WGE) & MtpKnB (ID of PDB: 2FUM). http://www. rcsb.org/pdb (RCSB Protein Data Bank (PDB) database) was used to retrieve the targeted enzyme.

4.1.4. Preparation of protein

Before starting the molecular docking, the water molecules were removed from the respective proteins. The selected enzymes from the protein data bank were subjected to Molegro viewer by which those enzymes were refined and their binding site was analyzed.

4.1.5. Preparation of ligand

The structures of ligands were drawn using Chem Draw software. The protein file (pdb) was being further optimized by adding hydrogen atoms and removing water molecules. The end up with all these procedures, the protein and ligand were well prepared for docking.

4.1.6. Grid box preparation and docking

Chem draw ultra was used to convert all files needed for the docking study. Parameters of the Grid box were fixed in such a way to permit for an appropriately-sized cavity space large sufficient to accommodate every analog within the binding site of each protein and were estimated using AutoDock Tools. Into the corresponding protein structures, entire co-crystallized inhibitory ligands are re-docked to allow comparison between docking scores and validate the accuracy. Based on their energy scores ligands are ranked and

http://dx.doi.org/10.29228/jrp.160
J Res Pharm 2022; 26(3): 625-640

searched at different orientations of ligands. Concerning its biological confirmation for each control ligand, a similar docking pose was obtained in the co-crystallized protein-ligand complex using our docking protocol. For each ligand best conformational space was explored with a 150 individual population size during the process of docking using the Lamarckian Genetic Algorithm. The rest of the parameters were fixed default. Some control inhibitors and the active binding sites of selected mycobacterial enzymes are well documented [30-33]. Docking efficiency was increased using a guided docking approach [34]. In this approach, in each protein binding site, each ligand conformation (including re-docking of the control inhibitors) was measured. Later, to forecast the top protein-ligand binding affinities scoring function was used to rank these conformations (Table 4 & Table 5). Highest predicted ligand/protein affinity was indicated by the lowest binding free energy. Biovia discovery studio visualizer was used to visualize the specific intermolecular interactions with the targets (Figure 1 & Figure 2).

4.2. Synthesis

*4.2.1. Synthesis of 4-(4-acetylbenzylidene)-2-methyloxazol-5(4H)-one (**ABO**)*

A mixture of 4-acetylbenzaldehyde (3.7 g, 0.025 moles), acetyl glycine (2.9 gm, 0.025 moles), anhydrous sodium acetate (1.5 gm), and acetic anhydride (5.9 ml) was heated at 110°C, with constant stirring. The mixture becomes almost solid, and then as the temperature rises, it gradually liquefies and turns deep yellow. After completion of the reaction monitored by TLC, the reaction is allowed to cool and ethanol (10 ml) is added slowly to the contents of the flask. After allowing the reaction mixture is left to stand overnight, the yellow color product is filtered and washed with ice-cold ethanol and finally with boiling water and recrystallized in ethanol to yield 4-(4-acetylbenzylidene)-2-methyloxazol-5(4*H*)-one (**ABO**) [26]. Yield (in %): 77. Yellow solid. Melting point (in °C): 156-158 (from ethanol). IR (KBr) cm^{-1}: 1246 (C-O-C stretching), 1625 (C=C stretching), 1640 (C=N stretching), 1753 (C=O stretching), 2946 (Aliphatic C-H stretching), 3011 (Aromatic C-H stretching), 3084 (Alkene =CH stretching). ^{1}H-NMR ($CDCl_3$, 300 MHz) δ ppm: 1.38 (s, 3H, CH_3 of oxazole), 2.82 (s, 3H, $COCH_3$), 6.82-7.76 (m, 4H, Aromatic C-H), 7.90 (s, 1H, =CH of oxazole). EI-MS (*m/z*): 229 (M^+). *Anal*. Calcd for $C_{13}H_{11}NO_3$: C, 68.11; H, 4.84; N, 6.11. Found: C, 68.32; H, 4.82; N, 6.13.

*4.2.2. Synthesis of 4-(4-(3-(substituted phenyl)acryloyl)benzylidene)-2-methyloxazol-5(4H)-one (**CBO1-CBO15**)*

4-(4-acetylbenzylidene)-2-methyloxazol-5(4*H*)-one (**ABO**) (2.29g, 0.01 moles) and various substituted benzaldehyde (0.01 moles) was dissolved in ethanol (25 ml). To this mixture, 10 % sodium hydroxide solution (catalytic quantity) was added slowly and stirred for 6 h in a magnetic stirrer. The resulting mixture was then poured into cold water (400 ml) with constant stirring and left overnight in the refrigerator. The precipitate obtained 4-(4-(3-(substituted phenyl)acryloyl)benzylidene)-2-methyloxazol-5(4*H*)-one (**CBO1-CBO15**) was filtered, washed, and recrystallized from ethanol.

*4-(4-(3-(4-Aminophenyl)acryloyl)benzylidene)-2-methyloxazol-5(4H)-one (**CBO1**):* Yield (in %): 78. Pale yellow crystals. Melting point (in °C): 281-283 (from ethanol). IR (KBr) cm^{-1}: 1251 (C-O-C stretching), 1615 (C=C stretching), 1649 (C=N stretching), 1752 (C=O stretching), 2903 (Aliphatic C-H stretching), 3028 (Aromatic C-H stretching), 3097 (Alkene =CH stretching), 3316 (N-H stretching). ^{1}H-NMR ($CDCl_3$, 300 MHz) δ ppm: 1.02 (s, 3H, CH_3 of oxazole), 4.63 (s, 2H, NH_2), 6.96-7.80 (m, 8H, Aromatic C-H), 8.14 (s, 1H, =CH of oxazole), 8.49 (d, 1H, COC<u>H</u>=CH), 8.71 (d, 1H, COCH=C<u>H</u>). EI-MS (*m/z*): 332 (M^+). *Anal*. Calcd for $C_{20}H_{16}N_2O_3$: C, 72.28; H, 4.85; N, 8.43. Found: C, 72.55; H, 4.87; N, 8.40. Similarly all other compounds **CBO2-CBO15** were characterized and the data were presented in supplementary materials.

*4.2.3. Synthesis of 4-(4-(5-(substituted phenyl)-4,5-dihydro-1H-pyrazol-3-yl)benzylidene)-2-methyloxazol-5(4H)-one (**PBO1-PBO15**)*

A mixture of 4-(4-(3-(substituted phenyl)acryloyl)benzylidene)-2-methyloxazol-5(4*H*)-one (**CBO1-CBO15**) (0.05 moles) and hydrazine hydrate (0.1 mole) were dissolved in N, N-dimethyl formamide (30 ml). The mixture was refluxed at 120-140 °C for a period of 12 h. The resulting mixture was cooled and then poured into cold water containing ice with constant stirring. The precipitate obtained 4-(4-(5-(substituted phenyl)-4,5-dihydro-1H-pyrazol-3-yl)benzylidene)-2-methyloxazol-5(4*H*)-one (**PBO1-PBO15**) was separated by filtration, dried over the filter paper, and recrystallized using alcohol.

*4-(4-(5-(4-Aminophenyl)-4,5-dihydro-1H-pyrazol-3-yl)benzylidene)-2-methyloxazol-5(4H)-one (**PBO1**):* Yield (in %): 79. Puff color needles. Melting point (in °C): 185-187 (from ethanol). IR (KBr) cm^{-1}: 1235 (C-O-C stretching), 1609 (C=C stretching), 1642 (C=N stretching), 1754 (C=O stretching), 2953 (Aliphatic C-H stretching), 3007 (Aromatic C-H stretching), 3098 (Alkene =CH stretching), 3341 & 3356 (N-H stretching). ^{1}H-NMR ($CDCl_3$, 300 MHz) δ ppm: 1.09 (s, 3H, CH_3 of oxazole), 2.07 (d, 2H, CH_2 of pyrazole), 3.71 (t, 1H, CH of

http://dx.doi.org/10.29228/jrp.160
J Res Pharm 2022; 26(3): 625-640

pyrazole), 4.55 (s, 2H, NH_2), 6.72-7.58 (m, 8H, Aromatic C-H), 7.79 (s, 1H, NH of pyrazole), 7.94 (s, 1H, =CH of oxazole). EI-MS (*m/z*): 346 (M^+). *Anal*. Calcd for $C_{20}H_{18}N_4O_2$: C, 69.35; H, 5.24; N, 16.17. Found: C, 69.09; H, 5.26; N, 16.22. Similarly, all other compounds **PBO2-PBO15** were characterized and the data were presented in supplementary materials.

4.3. Biological activities

4.3.1. Antitubercular activity

In to agar slants (Middle brook 7H11), every investigated drug/compound (10-fold serial dilutions) were incorporated with an OADC growth supplement. $H37R_V$ strain of *M. tuberculosis* inoculums was prepared by using fresh agar slants (Middle brook 7H11) containing an OADC growth supplement. About 10^7cfu/mL concentrate of *M. tuberculosis* was prepared by dilution to 10^{-2} by using 1 mg/ml in 0.05% W/V Tween 80 in saline. The bacterial suspension (5 µl) was spotted per ml of the drug (10-fold serial dilutions) in 7H11 agar tubes. For 28 days all the tubes were incubated at 37 °C. The control tubes containing $H37R_V$ alone were used to compare with the test compounds containing tubes or sample tubes. Active concentration of test compound is the concentration at which entire inhibition of colony takes place. The minimum concentration of drug necessary to inhibit bacterial growth completely was taken as MIC [35-36]. MIC of reference drug Isoniazid, Rifampicin, Ethambutol was compared with test derivatives. MIC of the target analogs and the reference compounds are presented in Table 6.

4.3.2. Antibacterial activity

The antibacterial potency of test derivatives was estimated using the agar dilution method. Standard strains of the microorganism were acquired from the ATCC (American type culture collection), Rockville, USA & the pathological strains were obtained from the microbiology department, GITAM University, Vishakhapatnam, India, The antibacterial activity of the test derivatives was tested against the below-mentioned strains of bacteria: *S. Aureus ATCC25923*, *B. subtilis ATCC 6051, S. Albus ATCC* 17900, *S. Epidermidis* ATCC 35984, M. *Luteus ATCC 10240*, *K. pneumoniae ATCC 13883, S. typhimurium ATCC 33068, P. vulgaris ATCC 9484, E. coli ATCC 2592,* & *P. aeruginosa ATCC 2853.* For bacterial growth Hi-media Muller–Hinton Agar plates were used (37 °C, 24 h). On agar plates the lowest concentration of drugs that inhibit the bacterial growth was considered as MIC, ignoring a faint haze / single colony produced by the inoculums. Ciprofloxacin was employed as a standard drug for comparing the MIC of synthesized derivatives [37]. MICs of standard & test drugs are tabulated in Table 6 which is estimated from a minimum of 3 different experiments in duplicate.

4.3.3. Antioxidant screening (DPPH radical scavenging activity)

Initially, buffered methanol (95% v/v) was prepared by mixing methanol (60 ml) and 0.1 mol/l acetate buffer (pH 5.5; 40 ml). Later, DPPH (31.54 mg) was dissolved in buffered methanol (95% v/v; 25 ml) in a volumetric flask (50 ml) and finally the volume was made using buffered methanol (95% v/v). This solution is a 1 mmol/l DPPH solution. Test derivatives (10 mg) were dissolved in 10 ml of suitable solvent to prepare 1000 µg/ml concentrated test solution. In a test tube, different volumes (0.2, 0.4, 0.6, 0.8, 1.0 m) of the test derivatives (**PBO1-PBO15**) were taken to produce different concentration test derivatives (200, 400, 600, 800, and 1000 µg/ml) and made the volume to 4 ml using distilled water. To each test tube, 1 ml of DPPH solution (1 mmol, 3.953×10^{-10} µg/ml) was added, shaken the resulting mixture, and kept for 30 min at 30 °C. At 517 nm spectrophotometrically measured the absorbance of the resulting mixture. For comparison, vitamin C (ascorbic acid) was used as a reference drug. Like test derivatives, ascorbic acid (10 mg) was dissolved in 10 ml of suitable solvent to prepare 1000 µg/ml concentrated ascorbic acid solution. In a test tube, different volumes (0.2, 0.4, 0.6, 0.8, 1.0 m) of the ascorbic acid (1000 µg/ml concentrated ascorbic solution) were taken to produce different concentrations of ascorbic acid (200, 400, 600, 800, and 1000 µg/ml) and made the volume to 4 ml using distilled water. To each test tube, 1 ml of DPPH solution (1 mmol, 3.953×10^{-10} µg/ml) was added, shaken the resulting mixture, and kept for 30 min at 30 °C. At 517 nm spectrophotometrically measured the absorbance of the resulting mixture. 1 ml of DPPH solution was mixed with buffered methanol was used as control and the absorbance of this control must be in the range 0.500 ± 0.040 [38-39]. The obtained results are presented in Table 7. As inhibition percentage, the anti-radical activity was expressed and it is estimated using the below-mentioned equation.

Inhibition Percentage = [(Absorbance control – Absorbance sample)/Absorbance control] × 100

.

http://dx.doi.org/10.29228/jrp.160
J Res Pharm 2022; 26(3): 625-640

Acknowledgments: Authors are thankful to the management of Shadan Womens College of Pharmacy, Hyderabad, Telangana, India & GITAM – Deemed to be University, Gandhi Nagar, Rushikonda, Visakhapatnam, Andhra Pradesh, India for providing necessary facilities to carry out the research work successfully.

Author contributions: Concept – S.S., R.S.; Design – S.S., R.S.; Supervision – R.S.; Resources – S.S., R.S.; Materials – S.S.; Data Collection and/or Processing – S.S.; Analysis and/or Interpretation – S.S., R.S.; Literature Search – S.S.; Writing – S.S.; Critical Reviews – R.S.

Conflict of interest statement: The authors declared no conflict of interest.

REFERENCES

[1] Janin YL. Antituberculosis drugs: ten years of research. Bioorg Med Chem. 2007; 15(7): 2479-2513. [CrossRef]

[2] Ibrahim M, Andries K, Lounis N, Chauffour A, Truffot-Pernot C, Jarlier V. Synergistic activity of R207910 combined with pyrazinamide against murine tuberculosis. *Antimicrob Agents Chemother*. 2007;51(3):1011-1015. [CrossRef]

[3] Iacobino A, Fattorini L, Giannoni F. Drug-resistant tuberculosis 2020: Where we stand. Appl Sci. 2020; 10(6): 2153. [CrossRef]

[4] Mirzayev F, Viney K, Linh NN, Gonzalez-Angulo L, Gegia M, Jaramillo E, Zignol M, Kasaeva T. World Health Organization recommendations on the treatment of drug-resistant tuberculosis 2020 update. Eur Respir J. 2021; 57: 2003300. [CrossRef]

[5] Kakkar S, Narasimhan BA. Comprehensive review on biological activities of oxazole derivatives. BMC Chem. 2019; 13(1): 1-24. [CrossRef]

[6] Borcea AM, Ionut I, Crisan O, Oniga O. An overview of the synthesis and antimicrobial, antiprotozoal, and antitumor activity of thiazole and bisthiazole derivatives. Molecules. 2021; 26(3): 624. [CrossRef]

[7] Kaspady M, Narayanaswamy VK, Raju M, Rao GK. Synthesis, antibacterial activity of 2, 4-disubstituted oxazoles and thiazoles as bioisosteres. Lett Drug Des Discov. 2009; 6(1): 21-28. [CrossRef]

[8] Tomi IHR, Tomma JH, Al-Daraji AHR, Al-Dujaili AH. Synthesis, characterization, and comparative study the microbial activity of some heterocyclic compounds containing oxazole and benzothiazole moieties. J Saudi Chem Soc. 2015; 19(4): 392-398. [CrossRef]

[9] Aguirre-Rentería SA, Carrizales-Castillo JJ, Corona MD, Hernández-Fernández E, Garza-González E, Rivas-Galindo VM, Arredondo-Espinoza E, Avalos-Alanís FG. Synthesis and in vitro evaluation of antimycobacterial and cytotoxic activity of new α, β-unsaturated amide, oxazoline and oxazole derivatives from L-serine. Bioorg Med Chem Lett. 2020; 30(9): 127074. [CrossRef]

[10] Shah SR, Katariya KD. 1, 3-Oxazole-isoniazid hybrids: Synthesis, antitubercular activity, and their docking studies. J Heterocycl Chem. 2020; 57(4): 1682-1691. [CrossRef]

[11] Mori M, Stelitano G, Chiarelli LR, Cazzaniga G, Gelain A, Barlocco D, Pini E, Meneghetti F, Villa S. Synthesis, characterization, and biological evaluation of new derivatives targeting MbtI as antitubercular agents. Pharmaceuticals. 2021; 14(2): 155. [CrossRef]

[12] Guerrero-Pepinosa NY, Cardona-Trujillo MC, Garzón-Castaño SC, Veloza LA, Sepúlveda-Arias JC. Antiproliferative activity of thiazole and oxazole derivatives: A systematic review of in vitro and in vivo studies. Biomed Pharmacother. 2021; 138: 111495. [CrossRef]

[13] Kumar G, Singh NP. Synthesis, anti-inflammatory, and analgesic evaluation of thiazole/oxazole substituted benzothiazole derivatives. Bioorg Chem. 2021; 107: 104608. [CrossRef]

[14] Zimecki M, Bąchor U, Mączyński M. Isoxazole derivatives as regulators of immune functions. Molecules. 2018; 23(10): 2724. [CrossRef]

[15] Shakya AK, Kaur A, Al-Najjar BO, Naik RR. Molecular modeling, synthesis, characterization, and pharmacological evaluation of benzo [d] oxazole derivatives as non-steroidal anti-inflammatory agents. Saudi Pharm J. 2016; 24(5): 616-624. [CrossRef]

[16] Katariya KD, Vennapu DR, Shah SR. Synthesis and molecular docking study of new 1, 3-oxazole clubbed pyridyl-pyrazolines as anticancer and antimicrobial agents. J Mol Struct. 2021; 1232: 130036. [CrossRef]

[17] Al-Soliemy AM, Sabour R, Farghaly TA. Pyrazoles and fused pyrimidines: Synthesis, structure elucidation, antitubercular activity, and molecular docking study. Med Chem (Shariqah (United Arab Emirates)) 2021; PMID: 33761862. [CrossRef]

[18] Jadhav SB, Fatema S, Sanap G, Farooqui M. Antitubercular activity and synergistic study of novel pyrazole derivatives. J Heterocycl Chem. 2017; 55(7): 1634-1644. [CrossRef]

[19] B'Bhatt H, Sharma S. Synthesis and antimicrobial activity of pyrazole nucleus containing 2-thioxothiazolidin-4-one derivatives. Arabian J Chem. 2017; 10: S1590-0S1596. [CrossRef]

[20] Kumar RS, Arif IA, Ahamed A, Idhayadhulla A. Anti-inflammatory and antimicrobial activities of novel pyrazole analogs. Saudi J Biol Sci. 2016; 23(5): 614-620. [CrossRef]

[21] Hassan SY. Synthesis, antibacterial and antifungal activity of some new pyrazoline and pyrazole derivatives. Molecules. 2013; 18(3): 2683-2711. [CrossRef]

[22] Alegaon SG, Alagawadi KR, Sonkusare PV, Chaudhary SM, Dadwe DH, Shah AS. Novel imidazo [2, 1-b][1, 3, 4] thiadiazole carrying rhodanine-3-acetic acid as potential antitubercular agents. Bioorg Med Chem Lett. 2012; 22(5): 1917-1921. [CrossRef]

[23] Parepally JMR, Mandula H, Smith QR. Brain uptake of nonsteroidal anti-inflammatory drugs: ibuprofen, flurbiprofen, and indomethacin. Pharm Res. 2006; 23(5): 873-881. [CrossRef]

[24] Wehenkel A, Fernandez P, Bellinzoni M, Catherinot V, Barilone N, Labesse G, Jackson M, Alzari PM. The structure of PknB in complex with mitoxantrone, an ATP-competitive inhibitor, suggests a mode of protein kinase regulation in mycobacteria. FEBS Lett. 2006; 580(13): 3018-3022. [CrossRef]

[25] Prisic S, Husson RN. Mycobacterium tuberculosis serine/threonine protein kinases. Microbiol Spectr. 2014; 2(5): 2-5. [CrossRef]

[26] Jung JE, Lee SY, Park H, Cha H, Ko W, Sachin K, Kim DW, Chi DY, Lee HS. Genetic incorporation of unnatural amino acids biosynthesized from α-keto acids by an aminotransferase. Chem Sci. 2014; 5(5): 1881-1885. [CrossRef]

[27] Ma XL, Chen C, Yang J. Predictive model of blood-brain barrier penetration of organic compounds. Acta Pharm Sin. 2005; 26(4): 500-512. [CrossRef]

[28] Mannhold R. Molecular drug properties-Measurement and prediction. Wiley-VHC Verlag GmbH & Co. KGaA Weinheim, Germany. 2008, pp. 30-35.

[29] Zhao YH, Le J, Abraham MH, Hersey A, Eddershaw PJ, Luscombe CN, Boutina D, Beck G, Sherborne B, Cooper I, Platts JA. Evaluation of human intestinal absorption data and subsequent derivation of a quantitative structure-activity relationship (QSAR) with the Abraham descriptors. J Pharm Sci. 2001; 90(6): 749-784. [CrossRef]

[30] Björkelid C, Bergfors T, Raichurkar AKV, Mukherjee K, Malolanarasimhan K, Bandodkar B, Jones TA. Structural and biochemical characterization of compounds inhibiting Mycobacterium tuberculosis pantothenate kinase. J Biol Chem. 2013; 288(25): 18260-18270. [CrossRef]

[31] Batt SM, Jabeen T, Bhowruth V, Quill L, Lund PA, Eggeling L, Alderwick LJ, Fütterer K, Besra GS. Structural basis of inhibition of Mycobacterium tuberculosis DprE1 by benzothiazinone inhibitors. Proceedings of the National Academy of Sciences. 2012; 109(28): 11354-11359. [CrossRef]

[32] Wehenkel A, Fernandez P, Bellinzoni M, Catherinot V, Barilone N, Labesse G, Jackson M, Alzari PM. The structure of PknB in complex with mitoxantrone, an ATP-competitive inhibitor, suggests a mode of protein kinase regulation in mycobacteria. FEBS Lett. 2006; 580(13): 3018-3022. [CrossRef]

[33] Luckner SR, Machutta CA, Tonge PJ, Kisker C. Crystal structures of Mycobacterium tuberculosis KasA show mode of action within cell wall biosynthesis and its inhibition by thiolactomycin. Structure. 2009; 17(7): 1004-1013. [CrossRef]

[34] Meng XY, Zhang HX, Mezei M, Cui M. Molecular docking: A powerful approach for structure-based drug discovery. Curr Comput Aided Drug Des. 2011; 7(2): 146-157. [CrossRef]

[35] National committee for clinical laboratory standards: Antimycobacterial susceptibility testing for M. tuberculosis. Proposed standards M_{24}-T. Villanova, PA: National Committee for clinical laboratory standards. 1995.

[36] Sriram D, Yogeeswari P, Dinakaran M, Thirumurugan R. Antimycobacterial activity of novel 1-(5-cyclobutyl-1, 3-oxazol-2-yl)-3-(sub)phenyl/pyridylthiourea compounds endowed with high activity toward multidrug-resistant Mycobacterium tuberculosis. J Antimicrob Chemother. 2007; 59(6): 1194-1196. [CrossRef]

[37] Hawkey PM, Lewis DA. Medical bacteriology: A practical approach Oxford University Press 1st edition. 1990; pp. 181-185.

[38] Hatano T, Kagawa H, Yasuhara T, Okuda T. Two new flavonoids and other constituents in licorice root: their relative astringency and radical scavenging effects. Chem Pharm Bull. 1988; 36(6): 2090-2097. [CrossRef]

[39] Sharma OP, Bhat TK. DPPH antioxidant assay revisited. Food Chem. 2009; 113(4): 1202-1205. [CrossRef]

http://dx.doi.org/10.29228/jrp.160
J Res Pharm 2022; 26(3): 625-640

Journal of Research in Pharmacy
Research Article

http://dx.doi.org/10.29228/jrp.160
J Res Pharm 2022; 26(3): 625-640